Investigation of thermal behaviour of hybrid nanostructures based on Fe_2O_3 and PAMAM dendrimers

Laura Madalina Popescu · Roxana Mioara Piticescu ·
Maria Stoiciu · Eugeniu Vasile · Roxana Trusca

Abstract Dendrimers or biofunctionalized dendrimers can be assembled onto magnetic iron oxide nanoparticles to stabilize or functionalize inorganic nanoparticles. Carboxylated poly(amidoamine) PAMAM dendrimers (generation 4.5) have been used for the synthesis of iron oxide nanoparticles, resulting nanocomposites with potential biomedical applications. The present paper aims to systematically investigate the thermal behaviour of nanostructured hybrids based on ferric oxide and PAMAM dendrimers, by differential scanning calorimetry (DSC) technique. The novelty consists both in synthesis procedure of hybrid nanostructures as well as in DSC approach of these nanocomposites. For the first time, we propose a new method to prepare Fe_2O_3—dendrimer nanocomposite, using soft chemical process at high pressure. Commercial PAMAM dendrimers with carboxylic groups on its surface were used. When high pressure is applied, polymeric structures suffer morphological changes leading to hybrid nanostructures' formation. In the same time, crystallinity of inorganic nanoparticles is provided. DSC results showed an increase in thermal stability of composites as compared to commercial dendrimers. This could be due to the formation of strong interactions between ferric oxide and carboxyl groups, as confirmed by Fourier transform infrared spectroscopy. Electron microscopy analysis (SEM/EDX) and size measurements were performed to demonstrate the existence of nanosized particles.

Keywords Fe_2O_3 · PAMAM dendrimers · DSC · FT-IR · Nanocomposite

Introduction

The field of Tissue Regeneration and Engineering has greatly evolved over the last years, mainly due to the combination of the important advances verified in Biomaterials Science and Engineering with those of Cell and Molecular Biology. In particular, a new and promising area arose—Nanomedicine—that takes advantage of the extremely small size and especially chemical and physical properties of nanomaterials, offering powerful tools for health improvement [1–3]. Dendrimers are a relatively new class of nanosized polymers with unique architectural, structural and functional features that recommends them for nano-biomedical applications such as bioimaging, drug and gene delivery, cancer diagnosis and sensors. Recently, dendrimer nanocomposites have attracted much interest for a variety of advanced applications in the field of nanomedicine due to their controlled composition, predetermined size, shape and optional surface functionalities [4–13].

Also, metal oxides-dispersed polymer nanocomposites have been extensively studied, since they exhibit interesting properties, including thermal resistance, with many applications in optical, magnetical and biomedical fields [14, 15].

As a result, polyamidoamine (PAMAM)–Fe_2O_3 nanocomposites have been developed for applications in

L. M. Popescu (✉) · R. M. Piticescu · M. Stoiciu
National R&D Institute for Non-Ferrous and Rare Metals,
102 Biruintei Blvd., Pantelimon, Ilfov, Romania
e-mail: mpopescu@imnr.ro

E. Vasile · R. Trusca
S.C. METAV C-D S.A, 31 C.A. Rosetti Str., Bucharest,
Romania

nanomedicine [16–18]. Strable et al. [7] and Shi et al. [19] synthesized carboxyl-terminated PAMAM dendrimers–iron oxide nanocomposites by a template technique for magnetic resonance imagining (MRI) applications. The multifunctional nanocomposites found to have unusually high T1 and T2 NMR relaxivities and could represent a new generation of contrast agents for MRI applications [18]. Wang et al. [20] reported the synthesis of the amino-terminated nanocomposites by electrostatic layer-by-layer self-assembly technique for specific targeting of cancer cells. In other work, super paramagnetic monodisperse nanoparticles (NP) of iron oxide 7.6 nm in size were modified with NH_2 terminated PAMAM G5 connected to fluorescent molecules and FA [21, 22]. The results have shown that these NPs were successfully absorbed with cancerous cells KB containing FA receptors.

In the present paper, an innovative synthesis route is proposed for the preparation of hybrid organic–inorganic nanocomposites based on Fe_2O_3 and carboxyl terminated PAMAM dendrimers:high pressure hydrothermal method. This procedure is a one-step soft chemical process which consists in in situ formation of Fe_2O_3 nanostructures in the presence of COOH terminated PAMAM dendrimers in a perfectly sealed autoclave under 20–100 atm Ar pressure. The thermal behaviour of nanostructured hybrids based on ferric oxide and PAMAM dendrimers is systematically investigated by differential scanning calorimetry (DSC) and thermal gravimetry (TG) analyses. It is expected that thermal stability of hybrid nanocomposites is higher than that of individual components.

Materials and methods

Materials

Iron(III) chloride hexahydrate was used as received from Merck, Germany.

PAMAM generation 2 dendrimer with 16 succinamic acid surface groups and 1,4-diaminobutane core, solution 10 wt% in H_2O (Linear formula: $[NH2(CH2)4NH2]$: $(G = 2)$; dendri $PAMAM(NHCOCH_2CH_2COOH)_{16}$) and PAMAM generation 6 dendrimer with 256 succinamic acid groups on its surface and 1,4-diaminobutane core, solution 10 wt% in H_2O (Linear formula: $[NH2(CH2)4NH2]$: $(G = 6)$; dendri $PAMAM(NHCOCH_2CH_2COOH)_{256}$) were used as received from Sigma Aldrich. Chemical structure of PAMAM G2 is presented in Fig. 1.

Ammonium hydroxide (NH_4OH) 25% solution (pure chemical reagent) was purchased from Chimopar, Romania and was used as 1:1 solution in water for iron oxide precipitation.
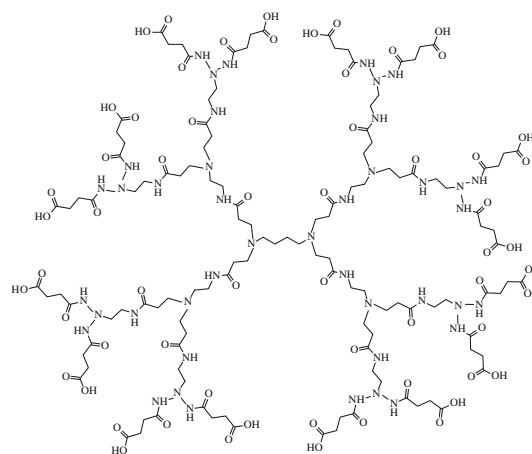

Fig. 1 Chemical structure of PAMAM G2 dendrimer with 1,4 diaminobutane core and 16 succinamic acid surface groups

Preparation of pure Fe_2O_3

Iron oxide was synthesized by the hydrothermal method under high-pressure conditions starting from commercial $FeCl_3$ powder (analytical grade) purchased from Merck and aqueous ammonia solution (25% w/w) used without further purification. The reagents were mixed in distilled water at room temperature and stirred continuously. This precursor suspension was placed in a 300 mL stainless steel autoclave for the hydrothermal reaction. After the reaction was completed, the resulting suspension was filtered and the precipitate washed several times with distilled water and dried in an oven in air at 100 °C.

Preparation of hybrid nanocomposites

Iron chloride hexahydrate and ammonia solution were vigorously mixed using a magnetic stirrer until a strong alkaline suspension with pH = 10 was obtained. PAMAM–succinamic acid dendrimer (solution 10 wt% in H_2O) was added and the mixture was transferred in Teflon vessel of CORTEST autoclave for hydrothermal reaction. High pressure was created inside the reaction system using an argon cylinder. The resulted suspension was lyophilized using a Martin Christ Alpha 1-2 LD Plus freeze dryer and analysed as presented below.

Characterization methods

Fourier transformed infrared spectroscopy

FTIR spectra of the PAMAM dendrimers, iron oxide and PAMAM–iron oxide nanocomposites (denoted as FeD) were recorded in the transmission mode on a ABB MB

3000 spectrometer between 4,000 and 550 cm^{-1} wavenumbers, and consisted of 64 scans at 4 cm^{-1} optical resolution. Standard IR grade KBr powder from Pike Technologies was used as reference. The spectra were recorded with the use of Horizon MB™ FT-IR software.

Scanning electron microscopy (SEM)

Morphological observations were carried out by electron microscopy using a HITACHI S2600N SEM coupled with an energy dispersive X-ray analyzer (EDX).

Thermal analysis

Thermal behaviour of the hybrid nanocomposites (FeD) was investigated using both TG and DSC analyses.

Thermogravimetric measurements of hybrid nanocomposites and iron oxide were performed on a SETARAM Setsys Evolution instrument (France). Data analysis was performed by the Setsoft 2000 software. Approximately 40 mg of each sample was examined in the temperature range 30–250 °C, in alumina crucible. The heating rate was 10^0 min^{-1}. Argon was used as carrier gas at a flow rate of 1 L h^{-1} during TG investigation.

A Netzsch DSC200 F3 Maia thermal analysis system (Germany) was used for calorimetric measurements of iron oxide–PAMAM dendrimers nanocomposites and its components. Data analysis was performed with the Proteus software. Approximately 15–20 mg of each sample was examined in the temperature range between −20 and 600 °C, in a covered Al crucible (three pin holes were applied in the cover). The heating rate was 10^0 min^{-1}. Argon was used as carrier gas at a flow rate of 1 L h^{-1} during the DSC investigation.

Results and discussions

FT-IR spectroscopy

FT-IR spectra of three representative samples (hybrid nanocomposites compared with initial PAMAM dendrimers) are presented in Fig. 2. The interactions between organic and inorganic components of the hydrothermally prepared nanostructures were studied using FT-IR spectroscopy. Figure 2 shows a representative FT-IR curve of PAMAM–succinamic acid dendrimer in comparison with FT-IR spectra of two selected hybrid nanocomposites (FeD) having different mass ratio and prepared at 100 atm.

The IR spectrum of pure PAMAM dendrimer shows characteristic peaks at 3,358 cm^{-1} (N–H stretching), 1,646 cm^{-1} (C=O asymmetric stretching vibration or amide I band) and 1,558 cm^{-1} (N–H bending vibration or
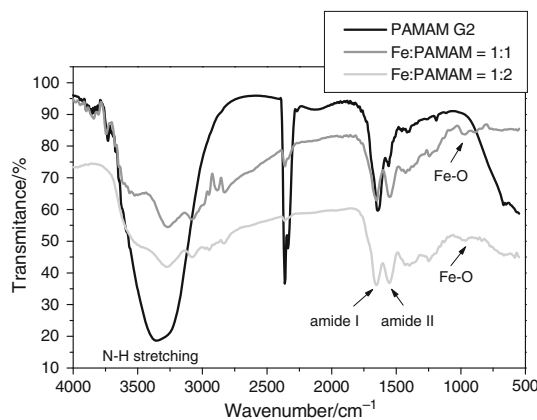
Fig. 2 FT-IR spectra of one PAMAM–succinamic acid dendrimer and Fe$_2$O$_3$–PAMAM nanostructures (Fe:PAMAM = 1:1 and 1:2 mass ratio)

amide II band). Almost identical spectra were observed for all PAMAM dendrimers used, irrespective of its generation. FT-IR spectra of FeD samples with different Fe:dendrimer mass ratio indicated the existence of both Fe–O (962, 894 and 838 cm^{-1}) and HN–C=O (1,650 and 1,550 cm^{-1}) molecular vibrations. Also, asymmetric stretching vibrations of CH$_2$ group from PAMAM dendrimers are observed in the range of 2,850–2,950 cm^{-1}. N–H stretching vibration band of the organic component could be overlapped by O–H group in the case of FeD samples. A narrow peak is observed at 3,270 cm^{-1} in all nanocomposite powders, which could be assigned to O–H stretching vibration.

SEM analysis

Scanning electron microscopy analysis was performed to demonstrate the existence of nanosized particles.

Small nanostructured particles of Fe$_2$O$_3$ of about 17-nm diameter were observed at the electronic microscope inside nanocomposite structures with 1:1 mass ratio Fe:PAMAM (Figs. 3, 4). In the EDX spectrum, it can be observed peaks corresponding to Fe, C and O, which demonstrates the existence of both components: iron oxide and dendrimer.

Thermal analysis

Thermogravimetric analyses were performed to evaluate thermal stability of nanostructured organic–inorganic composites prepared in high pressure conditions. Mass variations of some representative samples are presented in Table 1.

The mass loss of the unmodified iron oxide nanoparticles can be explained by desorption of water. On the other hand, the hybrid nanocomposites of iron oxide with PAMAM dendrimers may have lost their mass due to the

Fig. 3 SEM images of a representative iron oxide–PAMAM nanocomposite with 1:1 mass ratio Fe:PAMAM and corresponding EDX spectrum
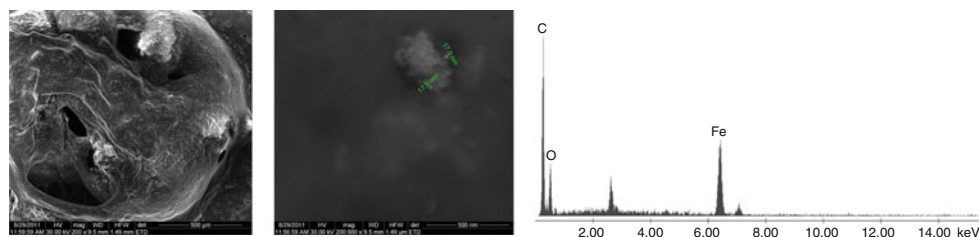

Fig. 4 SEM images of **a** iron oxide–dendrimer nanocomposite with 1:2 mass ratio (Fe:PAMAM), **b** pure Fe_2O_3 and its associated EDX spectrum
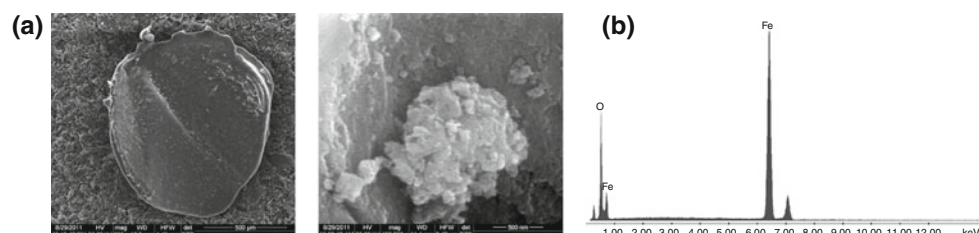
Table 1 Mass loss of pure iron oxide and hybrid Fe_2O_3–PAMAM samples in the temperature range 20–200 °C

Sample name	Composition (mass ratio)	Mass loss/%	Temperature range/°C
Fe_2O_3	Pure Fe_2O_3	15	20–200
FeD3	Fe:PAMAM G6 (1:1)	9.19	20–200
FeD4	Fe:PAMAM G6 (1:2)	14	20–200

dissociation and desorption of succinamic acid groups from the surface. The degree of mass loss corresponds to the proportion of dendrimer in nanocomposite material. A higher amount of PAMAM G6 leads to a higher percent of mass loss.

There is a small mass variation from room temperature to 200 °C in the case of hybrid nanostructures, mainly attributed to the decomposition of water and peripheral groups of the dendrimer (succinamic acid). Thermal behaviour of the hybrid Fe_2O_3–PAMAM nanocomposites also depends on the interactions between organic and inorganic components. Fe^{3+} ions could be bonded to surface carboxyl groups of the dendrimer or entrapped inside PAMAM cage. According to molecular dynamic simulation [23], most of Fe^{3+} ions are bound to the dendritic structure through COO^- groups but some of them are still free in the aqueous solvent. This leads to differences in

surface energies of the hybrid nanocomposite and substantial changes of the hydration–dehydration process. Unbounded carboxyl groups of PAMAM dendrimers are able to interact with the surrounding water. Lin et al. [24] found three classes of water:buried water well inside of the dendrimer surface, surface water associated with the dendrimer—water interface, and bulk water well outside of the PAMAM G5 dendrimer. They also found that water molecules are enthalpically favoured near the PAMAM dendrimers, but the net result was a thermodynamically unfavoured state of the water surrounding the PAMAM dendrimers. The excess free energy of the surface and buried waters is released when the PAMAM dendrimer binds to metal ions, providing an extra driving force.

It could be said that the thermal stability of iron oxide–PAMAM dendrimer composites increases compared to that of single dendrimer prepared in similar conditions ($T < 50$ °C and $P = 100$ atm). The results obtained by TG correlates well with those from DSC analysis. Peak temperatures and enthalpies of the individual components and hybrid nanocomposites measured experimentally using DSC technique are given in Table 2.

It can be observed that the temperature associated to water release increases in hybrid nanocomposites as compared to single dendrimer. The corresponding enthalpies are comparable for 1:1 mass ratio iron oxide–dendrimer

Table 2 Peak temperatures and enthalpies of the initial PAMAM dendrimers and hybrid nanocomposites

Sample name	Peak 1		Peak 2		Peak 3	
	T_1/°C	ΔH_1/J g^{-1}	T_2/°C	ΔH_2/J g^{-1}	T_3/°C	ΔH_3/J g^{-1}
PAMAM G2	59.5	81.46	187.1	7.42		
FeD2 (1:1 G2)	96.1	134.9			426.6	63.23
FeD3 (1:1 G6)	117.4	133.9	140.3	13.1	298	44.1
FeD4 (1:2 G6)	124.1	302.9			316.7	149.8

Fig. 5 DSC curves of **a** FeD3 (1:1), **b** FeD4 (1:2), **c** PAMAM–succinamic acid
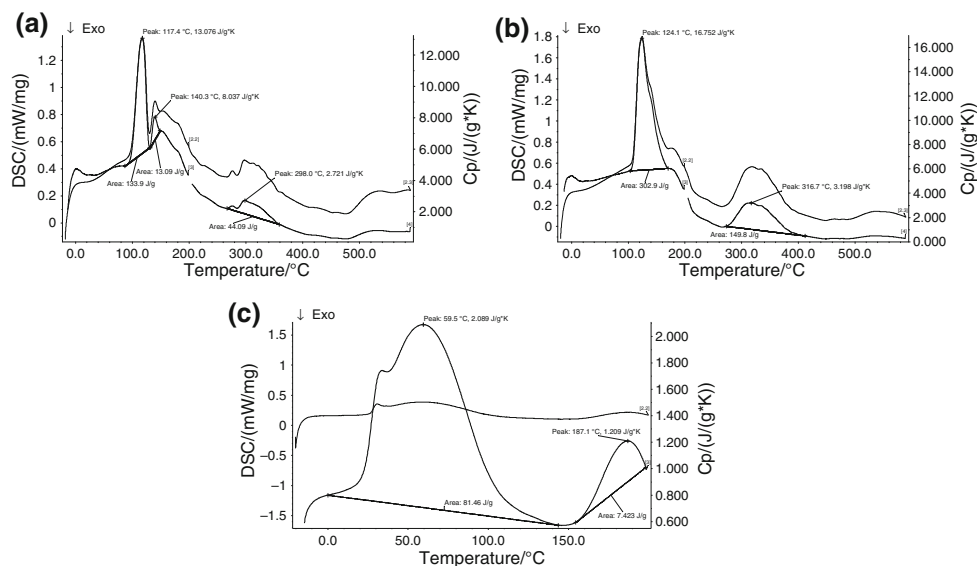
nanostructure irrespective of PAMAM generation, but ΔH increases dramatically when the dendrimers proportion in hybrid is double (Fe:PAMAM = 1:2). This is explained by the stronger surface energy of dendrimers which is able to bond water molecules from the surrounding medium. Peaks situated around 300 °C in FeD3 and FeD4 composites could be due to the melting of the organic part of hybrid structures and possible phase transformation of iron oxides.

Figure 5 shows DSC curves of nanostructured composites as compared to single PAMAM dendrimers with succinamic acid groups on its surface. The first endothermic peak observed at 117–124 °C in FeD samples (Fig. 5a, b) is due to the release of adsorbed water and is shifted to higher values compared to DSC curve of pure PAMAM (Fig. 5c). First endothermic peak of pure PAMAM dendrimers appears at 59.6 °C and it could be attributed to a form of molecular rearrangement, according to [25, 26]. A second endotherm developed in the case of samples with 1:1 mass ratio at 140 °C. Such thermal effect could be associated with a second stage of loss of adsorbed water or structural OH of the synthesized composites. A large endothermic peak occurs in FeD samples around 300 °C as a consequence of dendrimer melting and phase transformations: it can be assumed that this phase transformation corresponds to the formation of a structure with strong interactions between the organic and the inorganic component. Under the influence of pressure, intermolecular distances between these components decrease and the reactions of dendrimer with iron oxide is favored, leading to the formation of stable hybrid structures. This could explain the beginning of melting process at higher temperatures in composite samples as compared to single dendrimer where an endothermic peak attributed to melting is observed at 187 °C.

Higher values of specific heat capacities observed in the case of composites compared to single PAMAM dendrimer could be also due to the formation of stable structures with strong interactions between organic and inorganic part, in high pressure conditions. Further investigations are needed to define process kinetics and to confirm these assumptions.

Conclusions

Iron oxide–PAMAM nanocomposites were synthesized using an innovative route: in situ hydrothermal synthesis at high pressure and low temperature. It has been demonstrated that this synthesis procedure lead to nanostructured hybrid materials with improved thermal properties. Thermal behaviour of iron oxide nanocomposites with PAMAM G2 and PAMAM G6 were compared and it was found that peak temperature of the first thermal transformation is higher for hybrid samples with PAMAM G6 dendrimer. Thermal stability increases with increasing dendrimer generation and the reaction heat is higher when generation 6 of PAMAM is used.

Higher values of specific heat capacities observed in the case of composites compared to single PAMAM dendrimer could be due to the formation of stable structures with strong interactions between organic and inorganic part, in high pressure conditions. Further investigations are needed to define process kinetics and to confirm these assumptions.

Detailed studies will be done in the near future to optimize nanoparticles size for possible biomedical applications in drug delivery systems, medical diagnosis or hyperthermia, where chemically stable, well-dispersed and uniform-size particles are required.

References

1. da Silva Santos JL. Functionalization of dendrimers for improved gene delivery to mesenchymal stem cells. PhD Thesis, University of Madeira; (2009).

2. Kateb B, Chiu K, Black KL, Yamamoto V, Khalsa B, Ljubimova JY, Ding H, Patil R, Portilla-Arias JA, Modo M, Moore DF, Farahani K, Okun MS, Prakash N, Neman J, Ahdoot D, Grundfest W, Nikzad S, Heiss JD. Nanoplatforms for constructing new approaches to cancer treatment, imaging, and drug delivery: What should be the policy? NeuroImage. 2011;54:S106–24.

3. Sakamoto JH, van de Ven AL, Godin B, Blanco E, Serda RE, Grattoni A, Ziemys A, Bouamrani A, Hu T, Ranganathan SI, De Rosa E, Martinez JO, Smid CA, Buchanan RM, Lee S-Y, Srinivasan S, Landry M, Meyn A, Tasciotti E, Liu X, Decuzzi P, Ferrari M. Enabling individualized therapy through nanotechnology. Pharmacol Res. 2010;62:57–89.

4. Balogh L, Bielinska A, Eichman JD, Valluzzi R, Lee I, Baker JR, Lawrence TS, Khan MK. Dendrimer nanocomposites in medicine. Chem Today. 2002;20:35–40.

5. Barrett T, Ravizzini G, Choyke PL, Kobayashi H. Dendrimers in medical nanotechnology. Application of dendrimer molecules in bioimaging and cancer treatment. IEEE Eng Med Biol Mag. 2009;28:12–22.

6. Tomalia DA. Dendrimers: key properties of importance to nanomedicine. Nanomedicine. 2006;2:307.

7. Strable E, Bulte JWM, Moskowitz B, Vivekanandan K, Allen M, Douglas T. Synthesis and characterization of soluble iron oxide-dendrimer composites. Chem Mater. 2001;13:2201–9.

8. Saboktakin MR, Maharramov A, Ramazanov MA. Synthesis and characterization of MRI-detectable magnetic dendritic nanocarriers. Polym Plast Technol Eng. 2010;49:104–9.

9. Liu S, Lin Q, Zhang X, He X, Xing X, Lian W, Huang J. Electrochemical immunosensor for salbutamol detection based on CS–Fe_3O_4–PAMAM–GNPs nanocomposites and HRP_MWCNTs–Ab bioconjugates for signal amplification. Sens Actuators B. 2011;156:71–8.

10. Menjoge AR, Kannan RM, Tomalia DA. Dendrimer-based drug and imaging conjugates: design considerations for nanomedical applications. Drug Discov Today. 2010;15:171–85.

11. Mishra MK, Kotta K, Hali M, Wykes S, Gerard HC, Hudson AP, Whittum-Hudson JA, Kannan RM. PAMAM dendrimers-azithromycin conjugate nanodevices for the treatment of *Chlamydia trachomatis* infections. Nanomed Nanotechnol Biol Med. 2011;7:935–44.

12. Tse C, Zohdy MJ, Ye JY, O'Donnell M, Lesniak W, Balogh L. Enhanced optical breakdown in KB cells labelled with folate-targeted silver-dendrimer composite nanodevices. Nanomed Nanotechnol Biol Med. 2011;7:97–106.

13. Sekhon BS, Kamboj SR. Inorganic nanomedicine–part 2. Nanomed Nanotechnol Biol Med. 2010;6:612–8.

14. Gaur MS, Rathore BS, Singh PK, Indolia A, Awasthi AM, Bhardwaj S. Thermally stimulated current and differential scanning calorimetry spectroscopy for the study of polymer nanocomposites. J Therm Anal Calorim. 2010;101:315–21.

15. Lagashetty A, Vijayanand H, Basavaraja S, Bedre MD, Venkataraman A. Preparation, characterization, and thermal studies of γ-Fe_2O_3 and CuO dispersed polycarbonate nanocomposites. J Therm Anal Calorim. 2010;99:577–81.

16. Chang YL, Meng XL, Zhao YL, Li K, Zhao B, Zhu M, Li YP, Chen XS, Wang JY. Novel water-soluble and pH-responsive anticancer drug nanocarriers: doxorubicin–PAMAM dendrimer conjugates attached to superparamagnetic iron oxide nanoparticles (IONPs). J Colloid Interface Sci. 2011;363:403–9.

17. Baykal A, Toprak MS, Durmus Z, Senel M, Sozeri H, Demir A. Synthesis and characterization of dendrimer-encapsulated iron and iron-oxide nanoparticles. J Supercond Nov Magn. doi:10.1007/s10948-012-1454-z (published online: 09 February 2012).

18. Zhang Y, Liu J-Y, Yang F, Zhang Y-J, Yao Q, Cui T-Y, Zhao X, Zhang Z-D. A new strategy for assembling multifunctional nanocomposites with iron oxide and amino-terminated PAMAM dendrimers. J Mater Sci Mater Med. 2009;20:2433–40.

19. Shi XY, Thomas TP, Myc LA, Kotlyar A, Baker JR Jr. Synthesis, characterization, and intracellular uptake of carboxyl-terminated poly(amidoamine) dendrimer-stabilized iron oxide nanoparticles. Phys Chem Chem Phys. 2007;9:5712–20.

20. Wang SH, Shi XY, Van Antwerp M, Cao Z, Swanson SD, Bi XD, Baker JR Jr. Dendrimer-functionalized iron oxide nanoparticles for specific targeting and imaging of cancer cells. Adv Funct Mater. 2007;17:3043–50.

21. Landmark KJ, DiMaggio S, Ward J, Kelly C, Vogt S, Hong S, Kotlyar A, Myc A, Thomas TP, Penner-Hahn JE, Baker JR, Banaszak Holl MM, Orr BG. Synthesis, characterization, and in vitro testing of superparamagnetic iron oxide nanoparticles targeted using folic acid-conjugated dendrimers. ACS Nano. 2008;2:773–83.

22. Bronstein LM, Shifrina ZB. Nanoparticles in dendrimers: from synthesis to application. Nanotechnol Russ. 2009;4:576–608.

23. Popescu L-M, Piticescu RM, Doni G, Danani A. Interfacial interactions of Fe^{3+} with PAMAM dendrimer in different pressure conditions. Molecular dynamics. Rev Roum Chim; 2011.

24. Lin S-T, Maiti PK, Goddard WA III. Dynamics and thermodynamics of water in PAMAM dendrimers at subnanosecond time scales. J Phys Chem B. 2005;109:8663–72.

25. Hay G, Mackay ME, Hawker CJ. Thermodynamic properties of dendrimers compared with linear polymers: general observations. J Polym Sci Part B Polym Phys. 2001;39:1766–77.

26. Staszczuk P. Surface properties of nanoparticles. In: Brown ME, Gallagher PK, editors. Handbook of thermal analysis and calorimetry. Recent advances, techniques and applications, vol. 5. Amsterdam: Elsevier; 2008. p. 343–7.